Bispyrene/Surfactant-Assembly-Based Fluorescent Sensor Array for Discriminating Lanthanide Ions in Aqueous Solution

Shihuai Wang, Liping Ding,* Junmei Fan, Zhongxiu Wang, and Yu Fang

Key Laboratory of Applied Surface and Colloid Chemistry of Ministry of Education, School of Chemistry and Chemical Engineering, Shaanxi Normal University, Xi'an 710062, P. R. China

Ⓢ *Supporting Information*

ABSTRACT: Lanthanides are valuable nonrenewable resources and widely used in a variety of industries. Detection and identification of lanthanide ions are in high demand but challenging because of the similarity among lanthanide ions. In the present work, a fluorescent sensor array of three cationic bispyrene derivatives mixed with anionic surfactant assemblies was developed. The sensor array exhibits cross-reactive responses to lanthanide ions when tested in aqueous solution. The combination of fluorescence variations at both monomer and excimer emission of each of the bispyrene sensor elements

provides a six-signal recognition pattern for lanthanide ions. Principle component analysis illustrates that the sensor array could at least identify 6 of the 14 similar lanthanide ions including La^{3+}, Pr^{3+}, Nd^{3+}, Eu^{3+}, Ho^{3+}, and Er^{3+}. UV−vis absorption measurements rule out the possibility of binding lanthanides with fluorophores. Fluorescence titration experiments in both cationic and neutral surfactant aqueous solutions reveal that the three fluorophores show slight fluorescence responses to the lanthanide ions, indicating that electrostatic attraction between lanthanide ions and anionic surfactant plays an important role in the sensing behavior of the sensor array. Control experiments with divalent metal ions find no cross-reactive responses, suggesting that the stronger electrostatic interaction with trivalent lanthanide ions is responsible for the multiple fluorescence responses.

KEYWORDS: supramolecular assembly, pattern recognition, SDS, pyrene, sensing
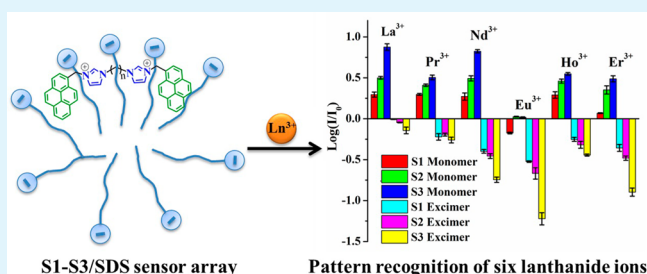
■ INTRODUCTION

Lanthanides are valuable nonrenewable resources and are widely used in petroleum catalysis,[1] agricultural fertilizer,[2] medical diagnostic,[3,4] and other fields because of their excellent optical, electrical, and magnetic characteristics.[5,6] The increased use of lanthanides has raised concern about their potential for pollution and demand for new detection methods.[7] A number of methods have been reported for the selective detection of lanthanide ions, which range from potentiometric membrane sensors,[8] to colorimetric gold nanoparticles,[7] to fluorescent molecular sensors,[9,10] and to fluorescent conjugated polymer sensors.[11] Compared to electrochemical and colorimetric methods, fluorescent sensors usually offer attractive advantages in terms of sensitivity, selectivity, availability of multiple sensing parameters, in vitro and/or in vivo measurement, in time, and online detection.[12,13]

However, although a huge amount of fluorescent sensors targeting heavy-metal ions have been developed over the past few decades,[14−16] highly sensitive and selective fluorescent sensors for the detection of lanthanide ions are still scarce and in high demand. The pioneering work of using fluorescent sensors for the detection of lanthanide ions was reported by Li and co-workers.[17] They synthesized a 1,4-diphenylethynylbenzene chromophore with 18-crown-6 moieties bound to the outer phenyl rings. The chromophore is luminescent, and its

fluorescence emission is quenched by lanthanide ions with larger ionic radii such as Ce^{3+}, Pr^{3+}, and Nd^{3+}. The selectivity of the fluorophore is provided by the utilization of crown ether moieties as receptors. A similar strategy was reported by Lianos and co-workers.[9] They used diazostilbene chromophore as the reporting element and modified it with a smaller size host, a benzo-15-crown-5 ether moiety, as the receptor for lanthanide ions. This fluorescent sensor displayed fluorescence off−on responses to Pr^{3+}, Nd^{3+}, and Eu^{3+}, which have smaller radii compared to those in the work by Li and co-workers. Recently, Crayston et al. reported using fluorescent conjugated polymers as selective sensors for Eu^{3+} and Tb^{3+}.[11] The presence of dibenzoylmethane and acetylacetonate ligands in the polymer backbone makes the conjugated polymers capable of binding the above two lanthanide ions and exhibiting different fluorescence behaviors. Das et al. reported a fluorescent ratiometric sensor containing a specially designed receptor for the selective detection of Nd^{3+} among other lanthanide ions.[10] However, the few reports on the fluorescent sensors for lanthanide ions were all conducted in organic solvents. Hence, in terms of practical applications, it is still challenging to

Scheme 1. Synthesis of Bispyrene Derivatives S1–S3 Containing Two Imidazolium Units
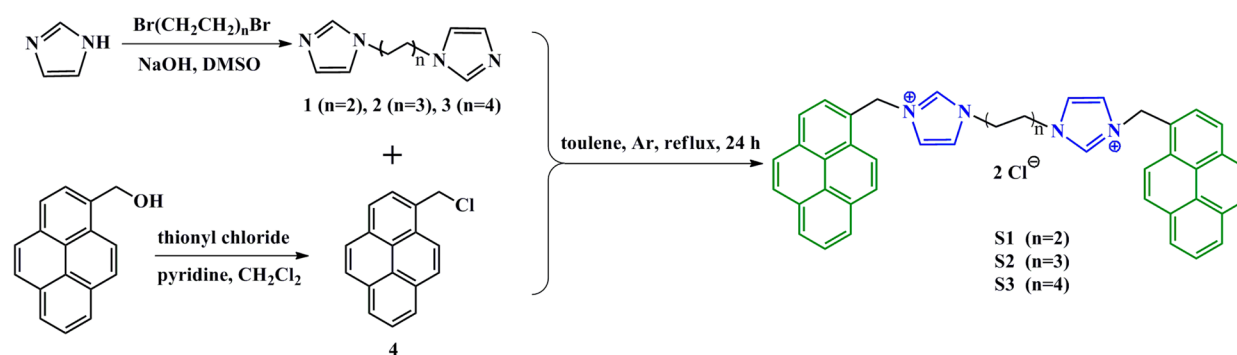
develop fluorescent sensors for measuring lanthanide ions in aqueous solution.

Amphiphilic surfactants usually form heterogeneous assemblies in water and provide hydrophobic microdomains to encapsulate hydrophobic compounds. This property of surfactant assemblies has been used to incorporate fluorescent molecular sensors to realize the aqueous detection of various metal ions like Hg^{2+},[13,18,19] Cd^{2+},[20] Cu^{2+},[21–23] Co^{2+},[24] etc. In addition, the use of surfactant assemblies could also modulate the photophysical properties and sensing behaviors of the encapsulated fluorescent molecule sensors.[25] For example, their sensitivities to metal ions could not only be enhanced by using surfactant micelles compared with a pure aqueous system[21] but also be easily modulated by varying the surfactant concentrations.[24,26] More interestingly, the target metal ions could also be tuned by varying the surfactant types. Bhattacharya and co-workers reported a pyrene-derivative-based fluorescent sensor that responds to both Cu^{2+} and Ni^{2+} in sodium dodecyl sulfate (SDS) micelles but only to Hg^{2+} in Brij-58 micelles.[27] Although the strategy of using surfactant assemblies encapsulating fluorescent molecular sensors has been widely used in the aqueous detection of heavy-metal ions, so far it has not been reported for applications in detecting lanthanide ions.

Therefore, in the present work, we aim to develop fluorescent molecular sensors to detect lanthanide ions in aqueous solution by using surfactant supramolecular assemblies. We have recently synthesized a cationic bispyrene fluorophore (**S1**; Scheme 1) and found that its mixtures with anionic surfactant aggregates display high sensitivity and selectivity toward Cu^{2+} and Co^{2+}.[24] The electrostatic interaction between the divalent metal ions and anionic surfactants is found to play an important role in adjusting the sensitivity and photophysical properties of the fluorophore. Herein, the trivalent lanthanide ions are expected to have a stronger electrostatic interaction with the anionic surfactant aggregates. In view of the high property similarity among lanthanide ions, we synthesized two more cationic bispyrene fluorophores (**S2** and **S3**; Scheme 1) with different spacer length and combined them with **S1** to construct a fluorescent sensor array. These three fluorophores were separately dissolved in the anionic SDS surfactant aggregates to build three fluorescent supramolecular assemblies. Their fluorescence responses to all of the lanthanide ions (except the radioactive one, Pm) were examined in aqueous solution and found to be cross-reactive to the presence of different lanthanide ions. The sensor array was found to be capable of discriminating at least six lanthanide ions using principle component analysis (PCA).

■ EXPERIMENTAL SECTION

Reagents. 1-Pyrenemethanol (98%), 1,4-dibromobutane (99%), 1,6-dibromohexane (98%), 1,8-dibromooctane (98%), and imidazole (>99%) were all purchased from Sigma-Aldrich and used without further purification. Sodium dodecyl sulfate (SDS), poly(ethylene glycol) sorbitan monooleate (Tween 80), and decyltrimethylammonium bromide (DTAB) were all of analytical grade and used as received. All lanthanide ions were used in nitrate salt and dissolved in water to obtain 0.25 mM stock solutions. SDS, Tween 80, and DTAB were dissolved in water to prepare aqueous solutions with the required concentrations. All aqueous solutions were prepared from Milli-Q water (18.2 MΩ cm at 25 °C).

Methods. The ^1H NMR and ^{13}C NMR spectra of the newly synthesized fluorophores were obtained on a Bruker Avance 400 MHz NMR spectrometer. The Fourier transform infrared spectra were measured on a Fourier transform infrared spectrometer (Vertex 70v; Bruker, Germany). The high-resolution mass spectrometry (HR-MS) spectra were acquired in elecrospray ionization (ESI) positive mode using a Bruker maxis UHR-TOF mass spectrometer. Fluorescence measurements were conducted at room temperature on a time-correlated single-photon-counting fluorescence spectrometer (FLS 920; Edinburgh Instruments, U.K.). UV–vis absorption spectra were recorded on a spectrophotometer (Lambda 950; PerkinElmer, USA).

Synthesis of Bispyrene Derivatives, S1–S3. The synthetic pathways used to obtain symmetric **S1–S3** are shown in Scheme 1. Diimidazole compounds (**1–3**) were first synthesized from imidazole and the corresponding α,ω-dibromoalkanes according to the procedures reported in the literature[28] but with minor modifications of the purification protocols (see the Supporting Information, SI). 1-Pyrenylmethyl chloride (**4**) was synthesized according to the method as described in the literature.[29] Subsequent reactions of **1–3** with 3 equiv of **4** produce the symmetric dicationic compounds with chloride counterions. The detailed synthesis process of **S1** was reported previously,[24] and those of **S2** and **S3** are described below.

A solution of **2** (0.15 g, 0.7 mmol) and **4** (0.53 g, 2.1 mmol) in 50 mL of dry toluene was refluxed for 24 h under argon. After cooling to room temperature, the formed precipitate was filtered and washed with anhydrous ether and acetone successively several times. After the resulting product was recrystallized twice with methanol, the final pure product containing two pyrene moieties and two charged imidazole units, **S2**, was obtained as a grayish powder (0.2 g, yield 41%). ^1H NMR (400 MHz, DMSO-d_6): δ 9.57 (s, 1H), 8.52 (d, J = 9.2 Hz, 1H), 8.38–8.06 (m, 8H), 7.88 (d, J = 24.5 Hz, 2H), 6.27 (s, 2H), 4.12 (t, J = 6.7 Hz, 2H), 1.71 (s, 2H), 1.17 (s, 2H). ^{13}C NMR (101 MHz, DMSO-d_6): δ 24.6, 28.9, 48.6, 49.9, 122.3, 122.6, 122.7, 123.6, 124.0, 125.1, 125.7, 125.7, 126.6, 127.2, 128.0, 128.5, 128.7, 130.0, 130.6, 131.4, 136.4. HR-MS (ESI; [M − Cl]⁺). Calcd for $C_{46}H_{40}N_4Cl$: m/z 683.2942. Found: m/z 683.2940.

Using a similar synthesis and purification protocol, **S3** was prepared by reacting **3** (0.15 g, 0.6 mmol) with **4** (0.45 g, 1.8 mmol) and purified to give the product (0.15 g, yield 33%). ^1H NMR (400 MHz, DMSO-d_6): δ 9.62 (s, 1H), 8.58–8.07 (m, 9H), 7.92 (d, J = 33.9 Hz, 2H), 6.29 (s, 2H), 4.12 (t, J = 6.9 Hz, 2H), 1.67 (d, J = 6.1 Hz, 2H),
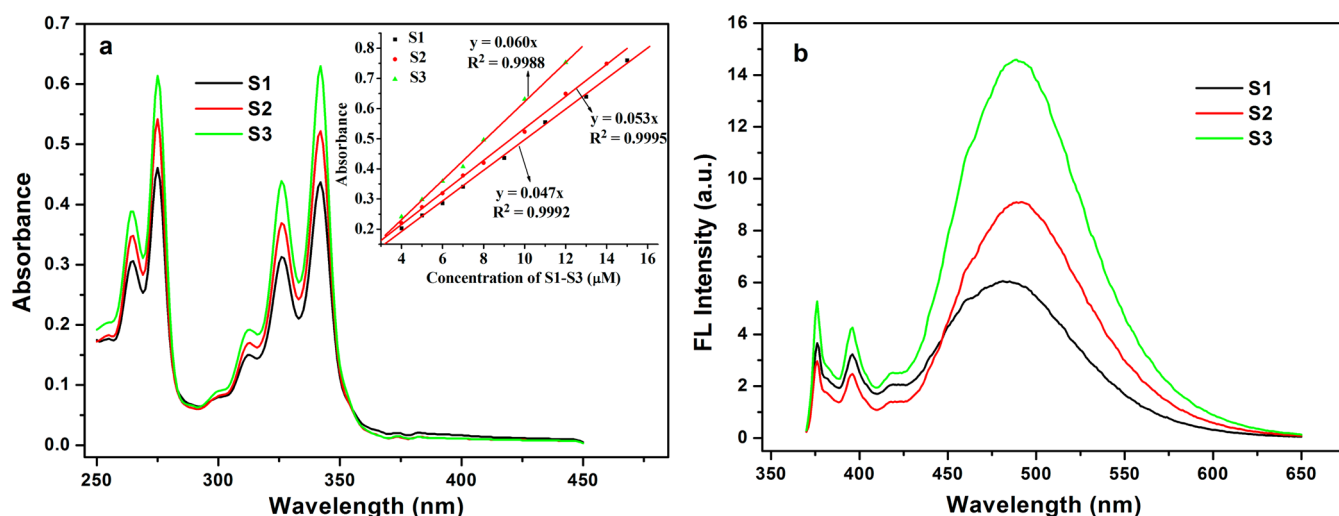
Figure 1. (a) UV−vis absorption spectra of **S1**−**S3** (10 μM) in methanol. Inset: Plots of UV−vis absorption of **S1**−**S3** in methanol as a function of the fluorophore concentration. (b) Steady-state fluorescence emission spectra of **S1**−**S3** (1.0 μM) in methanol (λ_{ex} =345 nm).
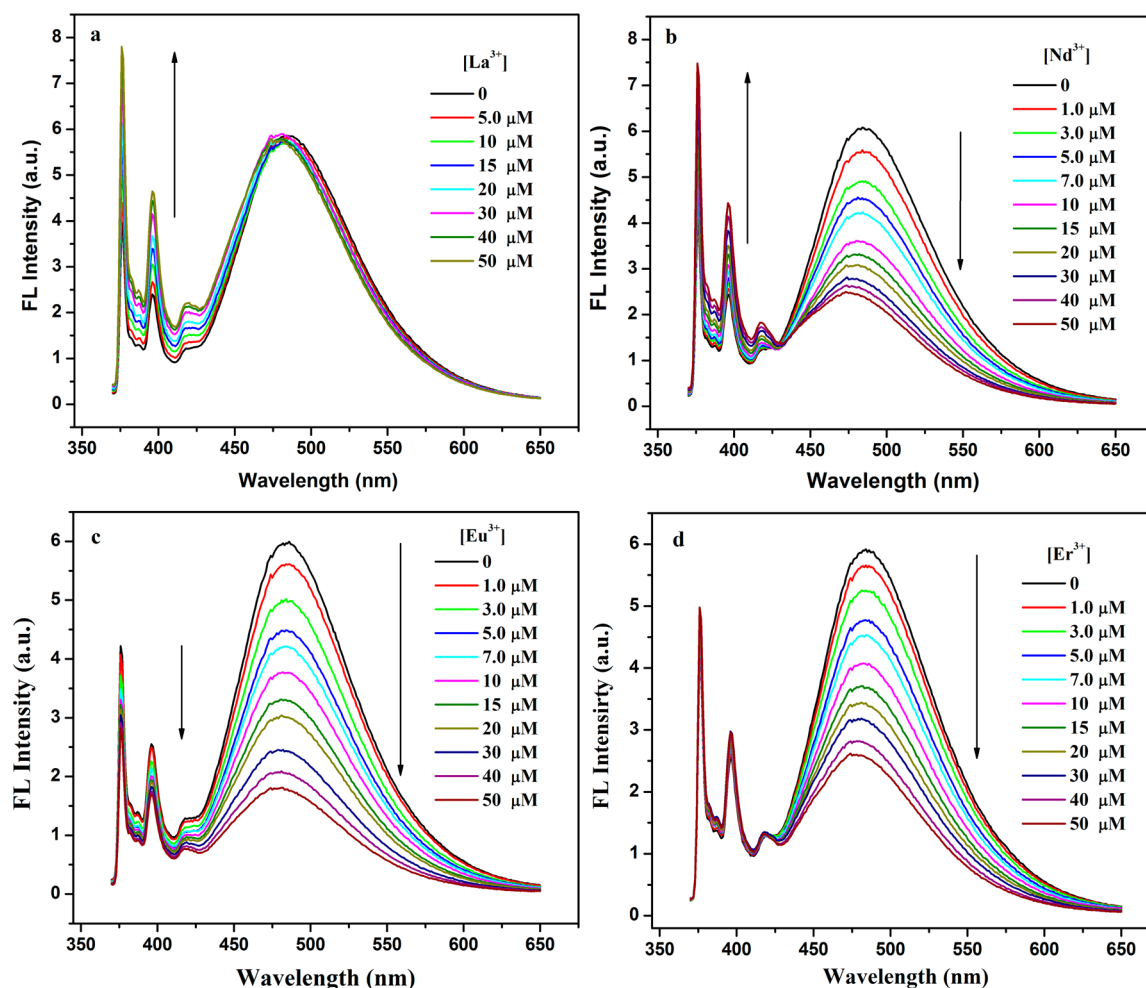

Figure 2. Fluorescence responses of the **S1**/SDS sensor system upon the titration of La^{3+} (a), Nd^{3+} (b), Eu^{3+} (c), and Er^{3+} (d) from 0 to 50 μM ([**S1**] = 1.0 μM; [SDS] = 4.0 mM; λ_{ex} = 345 nm).

1.08 (s, 4H). ^{13}C NMR (101 MHz, DMSO-d_6): δ 25.2, 27.9, 29.1, 48.7, 49.9, 122.4, 122.6, 122.6, 122.8, 123.6, 124.1, 125.2, 125.7, 125.9, 126.6, 127.2, 127.5, 128.0, 128.1, 128.5, 128.7, 130.6, 131.4, 136.3. HR-MS (ESI; [M − Cl]$^+$). Calcd for $C_{48}H_{44}N_4Cl$: m/z 711.3255. Found: m/z 711.3244.

■ RESULTS AND DISCUSSION

UV−Vis Absorption and Steady-State Fluorescence of S1−S3.
The UV−vis absorption of these bispyrene compounds (**S1**−**S3**) was measured in a good solvent, methanol, to evaluate the effect of the chain length. As seen in Figure 1a, the
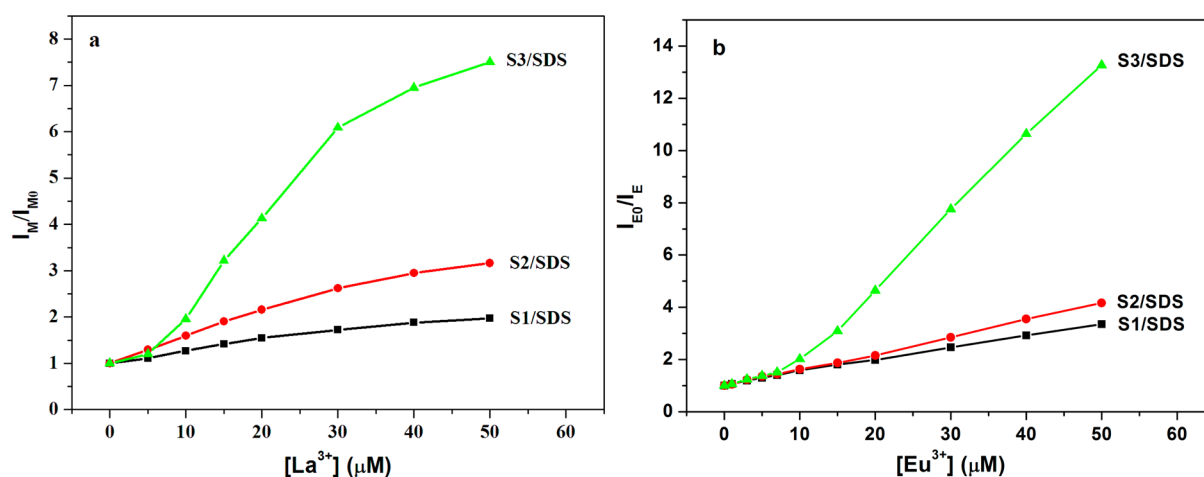
Figure 3. Fluorescence variation of **S1**−**S3**/SDS sensor systems upon the titration of La^{3+} (a) and Eu^{3+} (b) ([**S1**] = [**S2**] = [**S3**] = 1.0 μM; [SDS] = 4.0 mM; λ_{ex} = 345 nm).

three fluorophores display similar UV−vis absorption spectra with absorption peaks at 268, 278, 326, and 345 nm, which are typical for pyrene moieties.[30] As can be seen from the inset of Figure 1a, the plots of UV−vis absorption of the three fluorophores in methanol as a function of the fluorophore concentration are linear, following the equation $A = \varepsilon bc$. From the slopes of these plots, the extinction coefficients, ε (345 nm), of **S1**−**S3** were determined to be 4.70 (±0.01) × 10^4, 5.30 (±0.01) × 10^4, and 6.00 (±0.01) × 10^4 M^{-1} cm^{-1}, respectively. Apparently, the molar absorption coefficient is enhanced following growth of the chain length.

The steady-state fluorescence emission spectra of the three fluorophores (1.0 μM) in methanol were also measured. As shown in Figure 1b, **S1**−**S3** exhibit relatively weak monomer emission at shorter wavelengths and dominant broad excimer emission at longer wavelengths, which are characteristic emissions of pyrene moieties. Interestingly, the excimer emission intensity gradually increases with growth of the spacer chain length from **S1** to **S3**. Moreover, their fluorescence quantum yields (Φ) are also enhanced along the spacer chain length, which are determined to be 0.183, 0.215, and 0.247 for **S1**−**S3**, respectively. These results suggest that lengthening the spacer chain connecting the two charged imidazolium units strengthens both the absorption and emission ability of bispyrene fluorophores.

Sensing Behavior of S1−S3/SDS Assemblies as Sensor Platforms for Lanthanide Ions. Before systematic examination of the sensing behavior of **S1**−**S3**/SDS assemblies to lanthanide ions (Ln^{3+}) in aqueous solution, the SDS concentration effect on the sensitivity of the three fluorophores was first exploited. As was previously discovered for **S1**,[24] the fluorescence emission of **S2** and **S3** is also unstable in neat water and in a low-concentrated SDS aqueous solution. The fluorescence stability is greatly enhanced when the SDS concentration is or is larger than 4 mM. However, increasing the SDS concentration leads to a reduction of the sensitivity to Ln^{3+} for all three fluorophores. A typical fluorescence measurement result for **S3**/SDS solution systems with different SDS concentrations responding to Eu^{3+} and La^{3+} is illustrated in Figure S1 in the SI. Clearly, larger SDS concentration leads to remarkably reduced fluorescence sensitivity of **S3** to Ln^{3+}. Therefore, for these sensor systems, the SDS concentration was controlled at 4 mM because it provides better stability and

higher sensitivity for the fluorophores in responding to lanthanide ions. Moreover, the fluorescence quantum yields of **S1**−**S3** in 4 mM SDS aqueous solutions are determined to be 0.476, 0.510, and 0.548, respectively, and those in neat water are 0.209, 0.170, and 0.165, respectively. It was seen that the presence of SDS assemblies enhances the fluorescence quantum yields of all three fluorophores in water.

Then, the sensing behavior of each sensor/SDS assembly to 14 lanthanide ions, including La^{3+}, Ce^{3+}, Pr^{3+}, Nd^{3+}, Sm^{3+}, Eu^{3+}, Gd^{3+}, Tb^{3+}, Dy^{3+}, Ho^{3+}, Er^{3+}, Tm^{3+}, Yb^{3+}, and Lu^{3+}, was systematically examined. Interestingly, there are two characteristics that need to be specially noted. First, each sensor/SDS assembly displays different fluorescence responses to different Ln^{3+} ions. Figure 2 illustrates a representative result for the **S1**/SDS assembly as the sensor platform for Ln^{3+} ions, where there are four types of fluorescence responses to the measured Ln^{3+} ions. The first type is turn-on mode, where the fluorescence emission is enhanced upon titration of Ln^{3+} ions. Such a phenomenon is seen for the addition of La^{3+} to the **S1**/SDS sensor system, which produces only monomer enhancement (Figure 2a). The excimer emission shows slight intensity changes but blue shifts of the excimer maximum wavelengths from 484 nm in the absence of La^{3+} gradually to 474 nm in the presence of 50 μM of La^{3+}. Similar results were found for several other lanthanide ions including Ce^{3+}, Dy^{3+}, Gd^{3+}, Lu^{3+}, Sm^{3+}, Tb^{3+}, Tm^{3+}, and Yb^{3+} (data not shown). The second mode is ratiometric responses with monomer emission on and excimer emission off. This is observed for the titration of Nd^{3+} to the **S1**/SDS aqueous solution (Figure 2b). An isoemissive point at 430 nm between monomer and excimer emission is observed upon the titration of Nd^{3+}. Similar results are also surveyed upon the titration of Pr^{3+} and Ho^{3+} (Figure S2 in the SI). The third type is double turn-off mode, where both monomer and excimer emission decrease. This is observed for the gradual titration of Eu^{3+}. It can be seen that both monomer and excimer emission are quenched by the addition of Eu^{3+}, only to the extent that the excimer quenching is much larger than the monomer quenching (Figure 2c). The fourth type is single turn-off mode, where only excimer emission decreases. This phenomenon is observed for the addition of Er^{3+}. As seen in Figure 2d, the increasing addition of Er^{3+} induces only remarkable excimer quenching with slight monomer emission changes.

Interestingly, the fluorescence responses of the **S2**/SDS and **S3**/SDS systems to the above lanthanide ions are similar to that of the **S1**/SDS system. However, the responses of **S1**–**S3** to the same Ln^{3+} ion have some differences. This is the second characteristic of the sensor array. As an example to La^{3+} ion sensing, both **S2**/SDS and **S3**/SDS display the same monomer enhancement (Figure S3 in the SI) as that observed for **S1**/SDS (Figure 2a). Nevertheless, there are two differences among the three sensor systems. One is that the monomer-enhancing extent is increasing with increasing sensor spacer. As shown in Figure 3a, the increasing efficiency (I_M/I_{M0}) upon the addition of La^{3+} is increased along the order of **S1**/SDS < **S2**/SDS < **S3**/SDS, where I_{M0} and I_M are the monomer intensity at 376 nm in the absence and presence of lanthanide ions. The second is that the excimer responses to La^{3+} illustrate more variation from **S1** to **S3**. The excimer intensity starts to decrease upon the titration of La^{3+} for the **S2**/SDS system (Figure S3a in the SI) and decreases notably for the **S3**/SDS system with an isoemissive point (Figure S3b in the SI). Such a trend of enhancing fluorescence responses along the sensor length is also observed for other lanthanide ions. As illustrated in Figure S4 in the SI, the remarkable excimer quenching by Eu^{3+} is also witnessed for both **S2**/SDS and **S3**/SDS. The quenching efficiency (I_{E0}/I_E) of the excimer of three sensor systems is also increasing along the sensor spacer, as illustrated in Figure 3b, where I_{E0} and I_E are the fluorescence intensities at the excimer maximum of each sensor system in the absence and presence of Ln^{3+} ions. Therefore, the two characteristics of the array of **S1**–**S3**/SDS sensor systems for sensing lanthanide ions make it a good sensor array with cross-reactive responses. Thus, the combination of the three sensors, with each one providing two particular responses at both the monomer and excimer wavelengths, may generate a recognition pattern for the measured Ln^{3+} ions.

Pattern Recognition of Ln^{3+} of the Three-Element Sensor Array. The different fluorescence variations from both monomer and excimer emission of the three sensor systems indicate that emission at different wavelengths provides diverse responses toward different lanthanide ions. Thus, the fluorescence variation (I/I_0) of both the monomer at 376 nm and the excimer maximum emission for each sensor element to 14 lanthanide ions at 50 μM is collected. As a result, six fluorescence signals are combined for generating a recognition pattern for each Ln^{3+} ion. Because there is both fluorescence enhancement and quenching, the logarithm data of the fluorescence variation, $\log(I/I_0)$, are used for each fluorescence response signal. If $\log(I/I_0) > 0$, it means that fluorescence enhancement is observed, and if $\log(I/I_0) < 0$, it means that fluorescence quenching occurs. Figure 4 illustrates that the array of the three sensor systems each at two emission wavelengths can generate a six-signal fingerprint pattern toward six different lanthanide ions (La^{3+}, Pr^{3+}, Nd^{3+}, Eu^{3+}, Ho^{3+}, and Er^{3+}). The error bars represent the calculated standard deviation for three individual replicate measurements. The bar charts of the other eight lanthanide ions (Ce^{3+}, Sm^{3+}, Gd^{3+}, Tb^{3+}, Dy^{3+}, Tm^{3+}, Yb^{3+}, and Lu^{3+}) show patterns very similar to that of La^{3+} (see Figure S5 in the SI). These results suggest that the current three-element sensor array can generate a six-signal recognition pattern and discriminate 6 different lanthanide ions among the 14 tested lanthanide ions. As far as we know, this is the first report of a fluorescent sensor array based on surfactant assemblies for recognizing and discriminating multiple lanthanide ions.
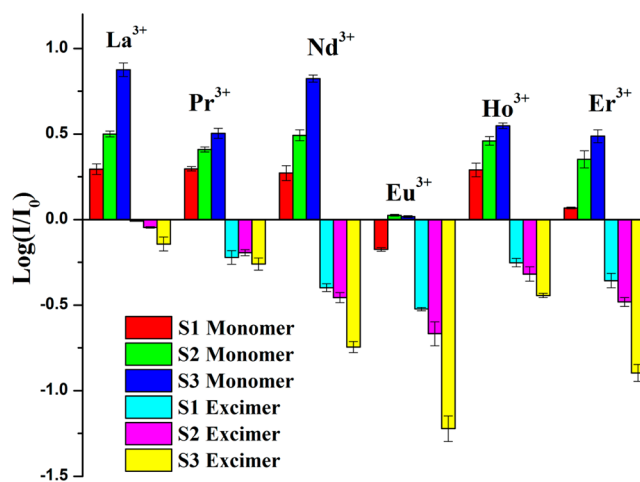

Figure 4. Recognition patterns for lanthanide ions (50 μM) by collecting logarithm data of fluorescence variations of **S1**–**S3** at selected monomer and excimer wavelengths in SDS aqueous solution ([**S1**] = [**S2**] = [**S3**] = 1.0 μM; [SDS] = 4.0 mM; λ_{ex} = 345 nm).

Discrimination Ability of the Sensor Array to Lanthanide Ions. To check the discrimination power of the sensor array composed of **S1**–**S3**/SDS systems, their fluorescence responses to the six representative Ln^{3+} ions at different concentrations, 5, 10, 15, 20, 30, and 40 μM, were measured. The logarithm data of the six fluorescence response signals, $\log(I/I_0)$, at the selected monomer and excimer wavelengths of three sensor systems were collected and analyzed by PCA. PCA is a classical statistical technique and has been widely used for sensor arrays to evaluate their discrimination ability.[31,32] Usually, it estimates combinations of variables in multidimensional data sets and then characterizes groupings of objects (classification) within the sets. This is achieved by calculating orthogonal eigenvectors (principal components, PCs) that lie in the direction of the maximum variance within that data.[33,34] The first PC contains the highest degree of variance, and other PCs follow in the order of decreasing variance. Thus, the PCA concentrates the most significant characteristics (variance) of the data into a lower dimensional space. For the present study, a weighted PCA method was used to classify the logarithm data (Table S1 in the SI). For this particular PCA analysis, the software *MATLAB R2010a* and weighting function $w(d_j) = (d_j/n)^{0.33}$ were used for PCA data processing, where d_j can be the Euclidean or Mahalanobis distance. The PCA obtained from the response data of a six-signal array requires only two dimensions to describe 98.9% of the variance. The two-dimensional PCA score plot is shown in Figure 5. It can be seen that the first principle component (PC1) carries about 95.09% of the variance, while the second principle component (PC2) carries ca. 3.81%. Altogether 98.9% of all of the variance in the data is carried by these two components. All of the tested lanthanide ions over the measured concentration range (5–40 μM) are grouped in well-separated clusters, illustrating the strong discrimination capability of the above-mentioned sensor array toward the six tested lanthanide ions.

To evaluate the feasibility of this sensor array in identifying different Ln^{3+} ions, we further measured the fluorescence responses of this sensor array to the six Ln^{3+} ions, which were prepared by a different person. These samples were used as known and unknown ones. The unknown ones were labeled as
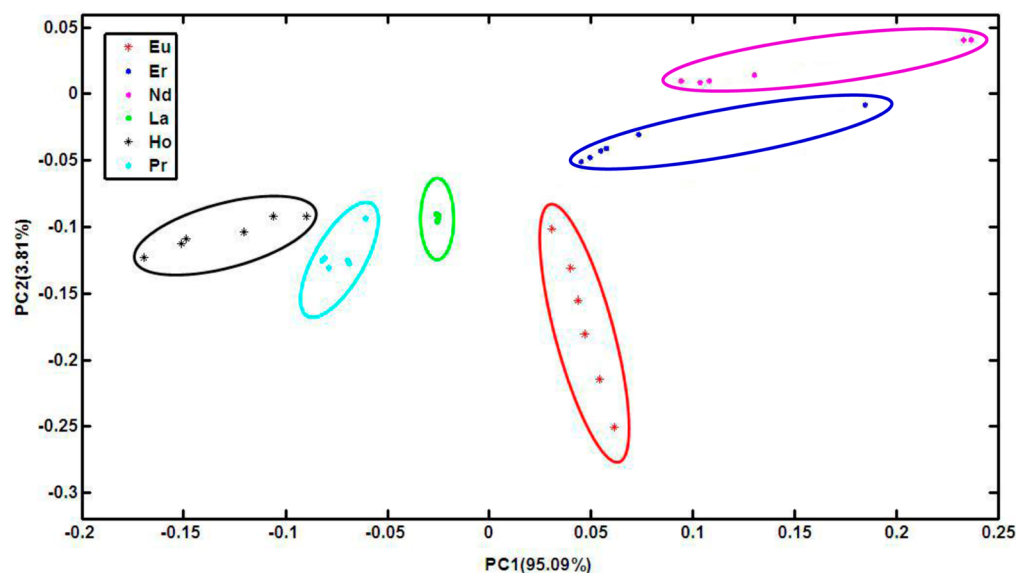
Figure 5. Two-dimensional PCA score plot for an array of **S1**−**S3**/SDS sensor systems discriminating lanthanide ions in aqueous solution at different concentrations ([**S1**] = [**S2**] = [**S3**] = 1.0 μM; [SDS] = 4.0 mM; [Ln^{3+}] = 5.0, 10, 15, 20, 30, and 40 μM).
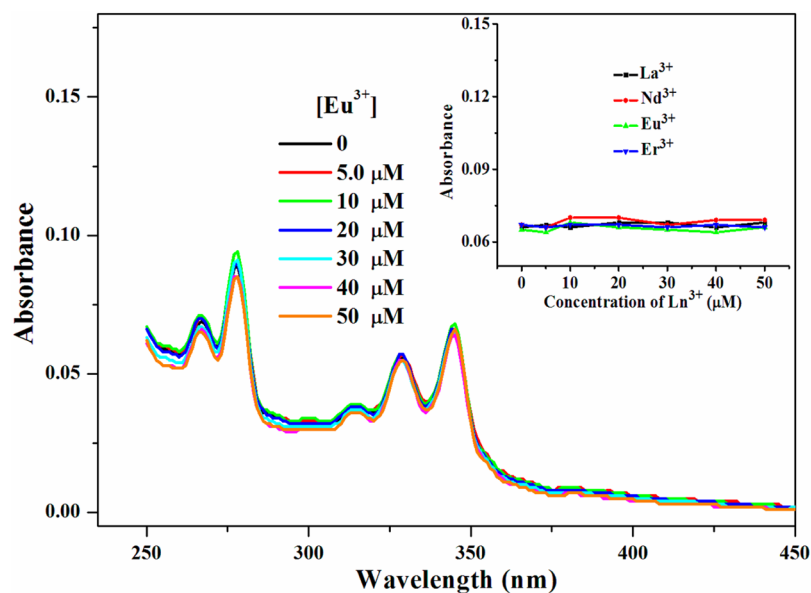
Figure 6. UV−vis spectra of **S3**/SDS aqueous solution upon the titration of Eu^{3+} from 0 to 50 μM ([**S3**] = 1.0 μM; [SDS] = 4.0 mM). Inset: UV−vis absorption intensity of the **S3**/SDS sensor system at 345 nm upon the titration of La^{3+}, Nd^{3+}, Eu^{3+}, and Er^{3+} from 0 to 50 μM.

U1, U2, ..., and U6. After collecting the logarithm data of the fluorescence variation (I/I_0) at the monomer and excimer emission for each sensor element (Table S2 in the SI), we used a similar PCA method to analyze these data for both the known and unknown samples. Delightedly, as shown in Figure S6 in the SI, the six unknown samples were well grouped with the six known samples. Also, as confirmed by the person who prepared the samples, the six unknown samples were correctly grouped with the same Ln^{3+} samples, indicating the feasibility of this method in recognizing different Ln^{3+} ions. We further used PCA to analyze the fluorescence responses of the sensor array to the six Ln^{3+} ions at concentrations lower than 5.0 μM (e.g., 1.0 and 3.0 μM) and found that the sensor array could not well discriminate them. This suggests that the detection limit of this method for discriminating Ln^{3+} is 5.0 μM, the lowest concentration used in Figures 5 and S6 in the SI.

Rationale for the Observed Sensing Behavior. To understand the sensing behavior of the sensor array to Ln^{3+} ions, several particular experiments were carried out to evaluate various effects. First, the UV−vis absorption spectra of three sensor systems were measured in the absence and presence of four representative lanthanide ions (La^{3+}, Nd^{3+}, Eu^{3+}, and Er^{3+}). Figure 6 displays the absorption spectra of **S3**/SDS assemblies, one of three sensor systems, upon the gradual titration of Eu^{3+}. It can be seen that the increasing addition of Eu^{3+} does not produce either an apparent spectral shift or an intensity variation of the sensor system. Moreover, as seen in the inset of Figure 6, the other three tested Ln^{3+} ions barely produce variation of the absorption intensity either. Similar results were also observed for **S1**/SDS and **S2**/SDS assemblies. No obvious spectral shift or intensity changes were seen in their UV−vis absorption under the same experimental conditions (data not
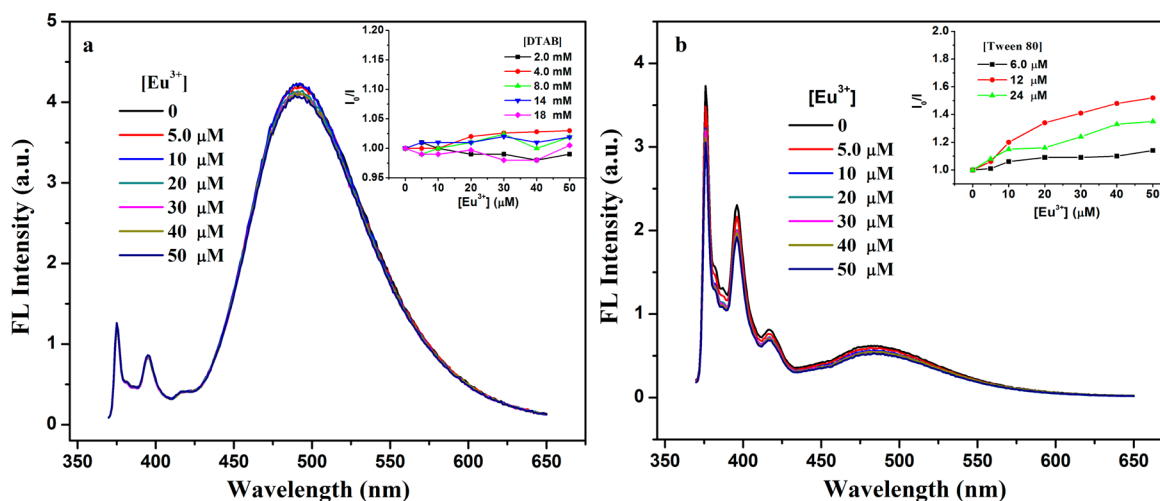
16161

dx.doi.org/10.1021/am504208a | ACS Appl. Mater. Interfaces 2014, 6, 16156−16165

Figure 7. (a) Fluorescence emission spectra of **S3**/DTAB upon the titration of Eu^{3+} ([**S3**] = 1.0 μM; [DTAB] = 4.0 mM). Inset: Excimer intensity variation of **S3** (1.0 μM) upon the titration of Eu^{3+} in different concentrated DTAB solutions (λ_{ex} = 345 nm). (b) Fluorescence emission spectra of **S3**/Tween 80 upon the titration of Eu^{3+} ([**S3**] = 1.0 μM; [Tween 80] = 6.0 μM). Inset: Excimer intensity variation of **S3** (1.0 μM) upon the titration of Eu^{3+} in different concentrated Tween 80 solutions (λ_{ex} = 345 nm).

shown). These results rule out the possibility of the three fluorescent sensor molecules forming complexes with these lanthanide ions.[24,26]

Second, we measured the sensing behavior of **S3** to lanthanide ions in the presence of two other different surfactant assemblies to evaluate the surfactant surface charge effect. The two surfactants used are Tween 80 as the neutral one and DTAB as the cationic one. Because the surfactant concentration may have an influence on the sensing behavior, the fluorescence responses of **S3** to four representative Ln^{3+} ions (Eu^{3+}, Er^{3+}, Nd^{3+}, and La^{3+}) were measured in the two surfactant solutions at a series of surfactant concentrations including those lower than the critical micelle concentration (CMC) and those above the CMC. It is known that the corresponding CMCs for DTAB and Tween 80 are 14 and 12 μM, respectively.[35,36] Therefore, the concentration of DTAB was controlled at 2, 4, 8, 14, and 18 mM, and that of Tween 80 was controlled at 6.0, 12, and 24 μM. Thus, the sensing behavior of **S3** in these two surfactant solutions could be thoroughly examined. Interestingly, the fluorescence of **S3** exhibits a slight variation upon titration of the four representative Ln^{3+} ions in all of the tested DTAB solutions. A sample result of the Eu^{3+} titration of **S3**/DTAB is shown in Figure 7a, where the DTAB concentration is 4 mM. It can be seen that the gradual addition of Eu^{3+} in this particular concentrated DTAB aqueous solution does not produce fluorescence quenching of **S3**. Moreover, as can be seen in the inset of Figure 7a, in either a higher or a lower concentrated DTAB solution, excimer emission of **S3** is barely quenched by the addition of Eu^{3+}, where fluorescence variation, I_0/I, is slightly fluctuating around 1. Similar results are observed not only for other Ln^{3+} ions such as Er^{3+}, Nd^{3+}, and La^{3+} (cf. Figure S7 in the SI) but also for the other two sensors, **S1** and **S2**, in all tested DTAB solutions (data not shown).

In the case of Tween 80 solutions, the titration of Ln^{3+} seems to produce some fluorescence variation. As displayed in Figure 7b, the gradual addition of Eu^{3+} leads to the fluorescence reduction of both monomer and excimer of **S3** in a 6.0 μM Tween 80 solution. Compared to that observed in 4 mM SDS systems, this fluorescence decrease is much smaller. Similar results are also observed for other Ln^{3+} ions such as Er^{3+}, Nd^{3+}, and La^{3+} in all tested Tween 80 solutions (cf. Figure S8 in the

SI). Moreover, the extent of fluorescence decrease, I_0/I, shows no relevant connection with the Tween 80 concentration (see the insets of Figures 7b and S8 in the SI). This fluorescence variation is more likely due to the instability of **S3** in the low-concentrated Tween 80 solutions. The control experiments in the absence of Ln^{3+} ions found that stirring only could produce similar fluorescence variation of **S3**/Tween 80 solutions.

The above results clearly reveal that the electrostatic interaction between Ln^{3+} ions and the surfactant plays an important role in producing the sensing behavior of the three sensors. Electrostatic attraction is expected to exist between Ln^{3+} ions and anionic SDS assemblies, which may draw Ln^{3+} ions close to the surface of the surfactant assemblies and produce fluorescence variation of the surfactant-surrounded fluorophores. However, in the presence of the cationic surfactant DTAB, electrostatic repulsion is supposed to occur between the positively charged lanthanide ions and cationic DTAB, which may inhibit the approach of lanthanide ions toward the surfactant assemblies and, as a result, produce a slight fluorescence variation of surfactant-surrounded fluorophores. For the neutral Tween 80 systems, electrostatic attraction is absent between Ln^{3+} ions and the nonionic surfactant. Similarly, the low approachability of lanthanide ions toward the Tween 80 assemblies makes it difficult for Ln^{3+} ions to influence the surfactant-assembly-encapsulated fluorophores.

In our previous work, **S1**/SDS exhibits a selective fluorescence quenching response to Cu^{2+} and Co^{2+} among a series of divalent metal ions, where the SDS concentration is also controlled at 4 mM.[24] However, multiple fluorescence variation modes are not observed for titration of these divalent metal ions. Similar results were also witnessed for the **S2**/SDS and **S3**/SDS sensor systems (Figure S9 in the SI), where only fluorescence quenching was observed for Cu^{2+} and Co^{2+}, and the other response modes observed for lanthanide ions are absent for the divalent metal ions. These results suggest that the stronger electrostatic interaction between Ln^{3+} ions and SDS assemblies may contribute to the cross-reactive responses of the three sensor/SDS systems. For measurement of the divalent metal ions, the electrostatic attraction between divalent metal ions and SDS assemblies only plays a role in attracting metal ions close to the sensor system and causing electron transfer

Scheme 2. Schematic Cartoon To Illustrate the Possible Mechanism of Ln³⁺ Ions Inducing Fluorescence Variation of the Cationic Bispyrene Fluorophores in SDS Assemblies
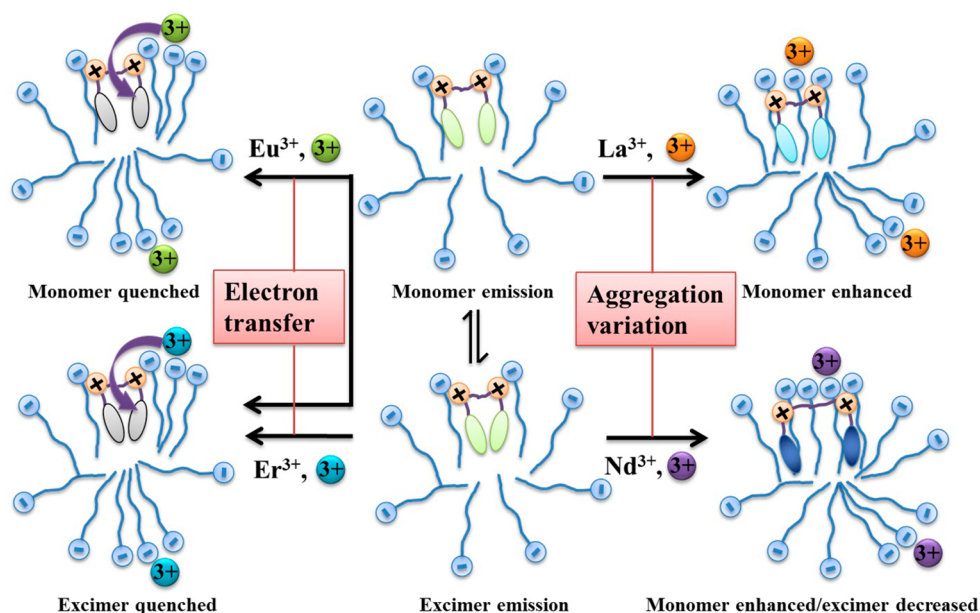
from metal ions to sensor fluorophores, which results in fluorescence quenching, whereas the conformation of the SDS assemblies is not so significantly affected and, as a result, a slight variation of the spatial location of the encapsulated fluorophore results. Differently, upon measurement of Ln³⁺ ions, the stronger electrostatic interaction between Ln³⁺ ions and anionic SDS assemblies not only draws Ln³⁺ close to the assemblies surface, which leads to electron transfer from Ln³⁺ to fluorophore and results in fluorescence quenching, but also produces more pronounced aggregation variation of the surfactant assemblies.[37]

We further measured the time-resolved emission spectra (TRES) of **S3** in both 4 mM SDS aqueous solution and a good solvent, methanol. Interestingly, the bispyrene fluorophore exhibits similar TRES in these two environments, where the formation of excimer is time-dependent and dynamic (Figure S10 in the SI).[38] This similarity to the results in a good solvent suggests that the environment for the cationic bispyrene in the SDS aggregation is more flexible. Therefore, the bispyrene fluorophore is more likely to exist at the flexible Stern layer of SDS aggregations than in the confined hydrophobic core. This could be reasonable because **S3** is cationic and the electrostatic interaction with a SDS headgroup may draw it to locate at the Stern layer. Therefore, the distance between and the geometry of the two pyrene moieties of the bispyrene fluorophore would be easily affected by SDS aggregation variation and lead to multiple fluorescence variation modes.[39]

On the basis of the above results and discussion, we proposed a possible mechanism for explaining the cross-reactive responses of **S1–S3**/SDS sensor systems to lanthanides (Scheme 2). As mentioned earlier, these cationic bispyrene fluorophores locate at the Stern layer of SDS aggregation. Because our sensor systems exhibit both strong monomer and excimer emission, there should be a dynamic balance for the two pyrene moieties between remaining as a separated monomer and encountering to form an excimer. After the addition of Ln³⁺ ions, these cationic trivalent ions were first attracted to the SDS aggregation surface because of

the electrostatic interaction between them and then caused multiple fluorescence variation modes. We believe two main processes are responsible for the different fluorescence responses. One is the electron-transfer process between Ln³⁺ and the aggregation-surface-located bispyrene fluorophores. This process is responsible for fluorescence quenching, which could be either monomer or excimer quenching. The other is the added Ln³⁺-induced surfactant aggregation variation, which further influenced the microenvironments of the bispyrene fluorophore or its conformation. Increased hydrophobic microenvironments may help to enhance monomer emission, and the enlarged distance between two pyrene moieties may induce an excimer decrease and an accompanied monomer enhancement. The difference in the radius and energy level of lanthanide ions may also contribute to the cross-reactive responses of the sensor array. However, the unregulated relationship between fluorescence responses and the lanthanide ions makes it diificult to thoroughly understand the role of the nature of lanthanide ions in the multiple response modes at the current stage.

■ CONCLUSION

In summary, we have shown that a cross-reactive sensor array can be constructed using three bispyrene derivatives with SDS assemblies (**S1–S3**/SDS assemblies). The three-element sensor array can produce a six-signal fingerprint pattern for lanthanide ions by combining fluorescence variation of both monomer and excimer of each sensor system. PCA analysis reveals that the current sensor array could discriminate 6 lanthanide ions (Eu³⁺, Er³⁺, Nd³⁺, La³⁺, Ho³⁺, and Pr³⁺) among 14 tested Ln³⁺ ions. UV–vis absorption studies show that there is no direct binding between Ln³⁺ ions and the three bispyrene fluorophores. Control experiments with different surfactants and divalent metal ions indicate that the electrostatic interaction between trivalent Ln³⁺ and anionic surfactants plays a role not only in attracting Ln³⁺ ions to the surfactant aggregate surface but also in altering the conformation of the surfactant assemblies. As a result, the binding of Ln³⁺ to

surfactant surfaces either quenches the fluorescence through electron transfer or alters the relative monomer and excimer emission by varying the spatial location of two pyrene moieties. This strategy of using surfactant supramolecular assemblies not only enables the bispyrene fluorophores to detect lanthanide ions in aqueous solution but also helps to modulate fluorescence emission and provide cross-reactive responses for developing fluorescent sensor arrays.

■ ASSOCIATED CONTENT

Ⓢ Supporting Information

Synthesis of compounds **1**–**3**, SDS concentration effect on the fluorescence responses of **S3** to Eu^{3+} and La^{3+}, fluorescence responses of an **S1**/SDS aqueous solution to Pr^{3+} and Ho^{3+}, fluorescence responses of **S2**/SDS and **S3**/SDS to La^{3+} and Eu^{3+}, recognition patterns of a sensor array to lanthanide ions, PCA analysis of unknown samples, fluorescence responses of **S3** to lanthanides in different concentrated DTAB solutions, fluorescence responses of **S3** to lanthanide ions in different concentrated Tween 80 solutions, fluorescence responses of **S2**/SDS and **S3**/SDS to divalent metal ions, and TRES of **S3** in SDS aqueous solution and methanol. This material is available free of charge via the Internet at http://pubs.acs.org.

■ AUTHOR INFORMATION

Corresponding Author

*Phone: +86-29-81530789. Fax: +86-29-81530727. E-mail: dinglp33@snnu.edu.cn.

Notes

The authors declare no competing financial interest.

■ ACKNOWLEDGMENTS

■ REFERENCES

(1) Seo, S.; Marks, T. J. Mild Amidation of Aldehydes with Amines Mediated by Lanthanide Catalysts. *Org. Lett.* **2007**, *10*, 317–319.

(2) Berton, M.; Mancin, F.; Stocchero, G.; Tecilla, P.; Tonellato, U. Self-Assembling in Surfactant Aggregates: An Alternative Way to the Realization of Fluorescence Chemosensors for Cu(II) Ions. *Langmuir* **2001**, *17*, 7521–7528.

(3) Bottrill, M.; Kwok, L.; Long, N. J. Lanthanides in Magnetic Resonance Imaging. *Chem. Soc. Rev.* **2006**, *35*, 557–571.

(4) Wooten, A. J.; Carroll, P. J.; Walsh, P. J. Insight into Substrate Binding in Shibasaki's $Li_3(THF)_n(BINOLate)_3Ln$ Complexes and Implications in Catalysis. *J. Am. Chem. Soc.* **2008**, *130*, 7407–7419.

(5) Ju, Q.; Tu, D.; Liu, Y.; Li, R.; Zhu, H.; Chen, J.; Chen, Z.; Huang, M.; Chen, X. Amine-Functionalized Lanthanide-Doped $KGdF_4$ Nanocrystals as Potential Optical/Magnetic Multimodal Bioprobes. *J. Am. Chem. Soc.* **2011**, *134*, 1323–1330.

(6) Wang, G.; Peng, Q.; Li, Y. Lanthanide-Doped Nanocrystals: Synthesis, Optical–Magnetic Properties, and Applications. *Acc. Chem. Res.* **2011**, *44*, 322–332.

(7) Lisowski, C. E.; Hutchison, J. E. Malonamide-Functionalized Gold Nanoparticles for Selective, Colorimetric Sensing of Trivalent Lanthanide Ions. *Anal. Chem.* **2009**, *81*, 10246–10253.

(8) Ganjali, M. R.; Ravanshad, J.; Hosseini, M.; Salavati-Niasari, M.; Pourjavid, M. R.; Baezzat, M. R. Novel Dy(III) Sensor Based on a New Bis-Pyrrolidene Schiff's Base. *Electroanalysis* **2004**, *16*, 1771–1776.

(9) Bekiari, V.; Judeinstein, P.; Lianos, P. A Sensitive Fluorescent Sensor of Lanthanide Ions. *J. Lumin.* **2003**, *104*, 13–15.

(10) Das, P.; Ghosh, A.; Das, A. Unusual Specificity of a Receptor for Nd^{3+} Among Other Lanthanide Ions for Selective Colorimetric Recognition. *Inorg. Chem.* **2010**, *49*, 6909–6916.

(11) Ritchie, J.; Ruseckas, A.; André, P.; Münther, C.; Van Ryssen, M.; Vize, D. E.; Crayston, J. A.; Samuel, I. D. W. Synthesis and Lanthanide-sensing Behaviour of Polyfluorene/1,10-phenanthroline Copolymers. *Synth. Met.* **2009**, *159*, 583–588.

(12) de Silva, A. P.; Gunaratne, H. Q. N.; Gunnlaugsson, T.; Huxley, A. J. M.; McCoy, C. P.; Rademacher, J. T.; Rice, T. E. Signaling Recognition Events with Fluorescent Sensors and Switches. *Chem. Rev.* **1997**, *97*, 1515–1566.

(13) Wang, J.; Qian, X.; Qian, J.; Xu, Y. Micelle-Induced Versatile Performance of Amphiphilic Intramolecular Charge-Transfer Fluorescent Molecular Sensors. *Chem.—Eur. J.* **2007**, *13*, 7543–7552.

(14) Gole, B.; Bar, A. K.; Mukherjee, P. S. Fluorescent Metal–organic Framework for Selective Sensing of Nitroaromatic Explosives. *Chem. Commun.* **2011**, *47*, 12137–12139.

(15) Zhang, J. F.; Lim, C. S.; Bhuniya, S.; Cho, B. R.; Kim, J. S. A Highly Selective Colorimetric and Ratiometric Two-Photon Fluorescent Probe for Fluoride Ion Detection. *Org. Lett.* **2011**, *13*, 1190–1193.

(16) Kim, H. N.; Ren, W. X.; Kim, J. S.; Yoon, J. Fluorescent and Colorimetric Sensors for Detection of Lead, Cadmium, and Mercury Ions. *Chem. Soc. Rev.* **2012**, *41*, 3210–3244.

(17) Xia, W.-S.; Schmehl, R. H.; Li, C.-J. A Fluorescent 18-Crown-6 Based Luminescence Sensor for Lanthanide Ions. *Tetrahedron* **2000**, *56*, 7045–7049.

(18) Avirah, R. R.; Jyothish, K.; Ramaiah, D. Dual-Mode Semisquaraine-Based Sensor for Selective Detection of Hg^{2+} in a Micellar Medium. *Org. Lett.* **2006**, *9*, 121–124.

(19) Zhao, Y.; Zhong, Z. Detection of Hg^{2+} in Aqueous Solutions with a Foldamer-Based Fluorescent Sensor Modulated by Surfactant Micelles. *Org. Lett.* **2006**, *8*, 4715–4717.

(20) Mameli, M.; Aragoni, M. C.; Arca, M.; Caltagirone, C.; Demartin, F.; Farruggia, G.; De Filippo, G.; Devillanova, F. A.; Garau, A.; Isaia, F.; Lippolis, V.; Murgia, S.; Prodi, L.; Pintus, A.; Zaccheroni, N. A Selective, Nontoxic, OFF–ON Fluorescent Molecular Sensor Based on 8-Hydroxyquinoline for Probing Cd^{2+} in Living Cells. *Chem.—Eur. J.* **2010**, *16*, 919–930.

(21) Ghosh, A. K.; Samanta, A.; Bandyopadhyay, P. Anionic Micelle-induced Fluorescent Sensor Activity Enhancement of Acridine Orange: Mechanism and pH Effect. *Chem. Phys. Lett.* **2011**, *507*, 162–167.

(22) Bag, S. S.; Kundu, R.; Talukdar, S. Fluorometric Sensing of Cu^{2+} Ion with Smart Fluorescence Light-up Probe, Triazolylpyrene (TNDMBPy). *Tetrahedron Lett.* **2012**, *53*, 5875–5879.

(23) Hu, X.-j.; Li, C.-m.; Song, X.-y.; Zhang, D.; Li, Y.-s. A New Cu^{2+}-selective Self-assembled Fluorescent Chemosensor Based on Thiacalix[4]arene. *Inorg. Chem. Commun.* **2011**, *14*, 1632–1635.

(24) Ding, L.; Wang, S.; Liu, Y.; Cao, J.; Fang, Y. Bispyrene/surfactant Assemblies as Fluorescent Sensor Platform: Detection and Identification of Cu^{2+} and Co^{2+} in Aqueous Solution. *J. Mater. Chem. A* **2013**, *1*, 8866–8875.

(25) Pallavicini, P.; Diaz-Fernandez, Y. A.; Pasotti, L. Micelles as Nanosized Containers for the Self-assembly of Multicomponent Fluorescent Sensors. *Coord. Chem. Rev.* **2009**, *253*, 2226–2240.

(26) Mallick, A.; Mandal, M. C.; Haldar, B.; Chakraborty, A.; Das, P.; Chattopadhyay, N. Surfactant-Induced Modulation of Fluorosensor Activity: A Simple Way to Maximize the Sensor Efficiency. *J. Am. Chem. Soc.* **2006**, *128*, 3126–3127.

(27) Kumari, N.; Dey, N.; Jha, S.; Bhattacharya, S. Ratiometric, Reversible, and Parts per Billion Level Detection of Multiple Toxic Transition Metal Ions Using a Single Probe in Micellar Media. *ACS Appl. Mater. Interfaces* **2013**, *5*, 2438–2445.

(28) Vlahakis, J. Z.; Mitu, S.; Roman, G.; Patricia Rodriguez, E.; Crandall, I. E.; Szarek, W. A. The Anti-malarial Activity of Bivalent Imidazolium Salts. *Biorg. Med. Chem.* **2011**, *19*, 6525−6542.

(29) Li, H.; Kitaygorodskiy, A.; Carino, R. A.; Sun, Y.-P. Simple Modification in Hexakis-Addition for Efficient Synthesis of C_{60}-Centered Dendritic Molecules Bearing Multiple Aromatic Chromophores. *Org. Lett.* **2005**, *7*, 859−861.

(30) Winnik, F. M. Photophysics of Preassociated Pyrenes in Aqueous Polymer Solutions and in Other Organized Media. *Chem. Rev.* **1993**, *93*, 587−614.

(31) Palacios, M. A.; Wang, Z.; Montes, V. A.; Zyryanov, G. V.; Anzenbacher, P. Rational Design of a Minimal Size Sensor Array for Metal Ion Detection. *J. Am. Chem. Soc.* **2008**, *130*, 10307−10314.

(32) Rochat, S.; Gao, J.; Qian, X.; Zaubitzer, F.; Severin, K. Cross-Reactive Sensor Arrays for the Detection of Peptides in Aqueous Solution by Fluorescence Spectroscopy. *Chem.—Eur. J.* **2010**, *16*, 104−113.

(33) Palacios, M. A.; Nishiyabu, R.; Marquez, M.; Anzenbacher, P. Supramolecular Chemistry Approach to the Design of a High-Resolution Sensor Array for Multianion Detection in Water. *J. Am. Chem. Soc.* **2007**, *129*, 7538−7544.

(34) Cao, Y.; Ding, L.; Wang, S.; Liu, Y.; Fan, J.; Hu, W.; Liu, P.; Fang, Y. Detection and Identification of Cu^{2+} and Hg^{2+} Based on the Cross-reactive Fluorescence Responses of a Dansyl-Functionalized Film in Different Solvents. *ACS Appl. Mater. Interfaces* **2013**, *6*, 49−56.

(35) Bahri, M. A.; Hoebeke, M.; Grammenos, A.; Delanaye, L.; Vandewalle, N.; Seret, A. Investigation of SDS, DTAB and CTAB Micelle Microviscosities by Electron Spin Resonance. *Colloids Surf., A* **2006**, *290*, 206−212.

(36) Chen, H.-R.; Chen, C.-C.; Reddy, A. S.; Chen, C.-Y.; Li, W. R.; Tseng, M.-J.; Liu, H.-T.; Pan, W.; Maity, J. P.; Atla, S. B. Removal of Mercury by Foam Fractionation Using Surfactin, a Biosurfactant. *Int. J. Mol. Sci.* **2011**, *12*, 8245−8258.

(37) Pereira, R. F. P.; Valente, A. J. M.; Burrows, H. D. Thermodynamic Analysis of the Interaction between Trivalent Metal Ions and Sodium Dodecyl Sulfate: An Electrical Conductance Study. *J. Mol. Liq.* **2010**, *156*, 109−114.

(38) Ding, L.; Bai, Y.; Cao, Y.; Ren, G.; Blanchard, G. J.; Fang, Y. Micelle-Induced Versatile Sensing Behavior of Bispyrene-Based Fluorescent Molecular Sensor for Picric Acid and PYX Explosives. *Langmuir* **2014**, *30*, 7645−7653.

(39) Wegner, S. V.; Okesli, A.; Chen, P.; He, C. Design of an Emission Ratiometric Biosensor from MerR Family Proteins: A Sensitive and Selective Sensor for Hg^{2+}. *J. Am. Chem. Soc.* **2007**, *129*, 3474−3475.

16165

dx.doi.org/10.1021/am504208a | *ACS Appl. Mater. Interfaces* 2014, 6, 16156−16165